Penerbit Akademia Baru

Journal of Advanced Research in Micro and Nano Engineering

Journal homepage:
https://www.akademiabaru.com/submit/index.php/armne/index
ISSN: 2756-8210

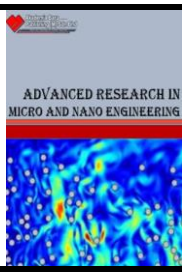

Innovative Nanodelivery Systems Transform Tuberculosis Treatment with Pyrazinamide-loaded Chitosan Nanoparticles

Pooneh Kia[1], Mohd Zobir Hussein[2], Umme Ruman[1], Ariyati Retno Pratiwi[2], Norazalina Saad[3], Zahra Izadi[4], Kamyar Shameli[5,*]

[1] Institute of Bioscience, Universiti Putra Malaysia, 43400 Serdang, Selangor, Malaysia
[2] Faculty of Dentistry, Universitas Brawijaya, Malang, Indonesia
[3] Cancer research laboratory, Institute of Bioscience, Universiti Putra Malaysia, 43400 Serdang, Selangor, Malaysia
[4] Department of Chemistry, Faculty of Science, Universiti Malaya, Kuala Lumpur 50603, Malaysia
[5] School of Medicine, Institute of Virology, Technical University of Munich, 81675 Munich, Germany

ARTICLE INFO

Article history:
Received 23 January 2024
Received in revised form 8 March 2024
Accepted 5 April 2024
Available online 30 May 2024

Keywords:
Chitosan nanoparticle; ethambutol; tuberculosis; nanodelivery formulation

ABSTRACT

Tuberculosis (TB) stands as an enduring and formidable global health challenge, necessitating innovative methodologies to optimize therapeutic outcomes. Within this context, nanotechnology emerges as a promising modality to augment TB therapy by enabling targeted drug delivery of anti-TB agents to infect cells, thereby maximizing therapeutic efficacy while mitigating adverse effects. This study focalizes on the synthesis of chitosan nanoparticles (CSNP) as a nanocarrier for the concurrent delivery of Pyrazinamide (PYR), a pivotal antibiotic in the first-line treatment of TB. The primary objective is to overcome challenges related to the limited solubility and bioavailability of these drugs, which hinder their effectiveness and pose toxicity risks. The encapsulation of PYR within CS proves advantageous, enhancing solubility, bioavailability, and targeted drug delivery. The resulting nanocarrier, denoted as CS-PYR, is prepared through ionic gelation, involving cross-linking chitosan-loaded anti-TB carriers with tripolyphosphate to achieve nanoscale dimensions. Various analytical techniques, including XRD, FTIR, TGA, TEM, FESEM, DLS, UV-vis spectroscopy, antibacterial assays, and cytotoxic MTT assays, are utilized for a comprehensive investigation. The spherical morphology of PYR-CSNP, with an average diameter of 60 to 100 nm, is confirmed by FESEM, TEM, and DLS analyses. FTIR and XRD analyses validate the successful fabrication and multifunctional properties of PYR incorporated into the CSNP matrix. The drug-loaded CSNP exhibits improved thermal stability, displaying decomposition between 200-400°C, indicating higher temperature resistance and greater weight loss compared to the CSNP carrier due to PYR inclusion. Drug release studies show sustained release behaviour, with 90-99% release in an acidic (pH 4.8) buffer solution over seven days, following a pseudo-second-order model. Moreover, the CS-PYR nanocarrier demonstrates superior efficacy against Gram-negative and Gram-positive bacteria, attributed to drug intercalation resulting in larger inhibition zones. Cytotoxicity assessments for CS-PYR indicate 80% cell viability in MRC5 cells, underscoring the nanocarrier's potential as a safe and effective TB treatment delivery system without adversely affecting normal cells. These findings position CS-PYR as a promising nanodelivery system for TB therapy, offering enhanced precision in drug delivery and safety.

* *Corresponding author.*
E-mail address: kamyar.shameli@tum.de

https://doi.org/10.37934/armne.19.1.2237

1. Introduction

Tuberculosis, a contagious respiratory ailment, presents challenges for conventional drug delivery systems in accurately targeting therapeutic agents [1]. Chitosan nanoparticles have recently emerged as a promising solution, demonstrating potential in enhancing drug efficacy, prolonging therapeutic effects, reducing drug resistance, dosage frequency, and ultimately improving patient adherence [2]. The transformative capabilities of nanoparticles in molecular manipulation have revolutionized drug delivery [3]. Chitosan nanoparticles, distinguished by their biodegradability, biocompatibility, stability, low toxicity, and facile preparation, constitute integral tools in modern drug delivery across diverse applications, including parenteral and per-oral administration, gene delivery, vaccine delivery, ocular drug delivery, brain targeting, stability enhancement, and controlled drug release [4]. Pyrazinamide (PYR), a potent anti-TB drug with patients needing to consume approximately 500 mg of YR on a daily basis, faces limitations due to reported side effects such as liver injury, anorexia, malaise, skin rashes and drug resistance. Its utility in latent TB treatment is restricted owing to pronounced liver toxicity [5]. Biocompatible, biodegradable drug delivery systems exhibiting sustained-release properties can significantly enhance drug bioavailability, thereby improving therapeutic efficacy, reducing dosing frequency, and mitigating a critical factor contributing to TB treatment failure.

Encapsulating anti-tubercular drugs in chitosan nanoparticles demonstrates an impressive ability to efficiently enter infected cells and release drugs precisely at the targeted site. Chitosan's strength as a nanocarrier lies in its effective bonding with anti-tubercular drugs at both ionic and molecular levels. The charged nature of chitosan enables the formation of stable complexes with drug ions, thereby improving overall drug loading capacity [6]. Once at the target site, chitosan-based nanocarriers interact with the surrounding environment, initiating controlled drug release mechanisms [7]. The reactive amino groups in chitosan molecules establish bonds with infected cells and macrophages, facilitating precise drug delivery [8]. This intricate interaction between chitosan and drugs ensures a sustained and controlled release, optimizing therapeutic outcomes while minimizing potential side effects. Encapsulating anti-tubercular drugs within chitosan nanocarriers not only enhances drug stability and effectiveness but also holds great promise in bolstering the fight against infection when incorporating the drug [9]. This study introduces an innovative anti-tuberculosis nanodelivery formulation utilizing CSNP as the carrier and PYR as the therapeutic agent through the ion gelation method. The formulation underwent comprehensive characterization employing XRD, FTIR, TEM, and UV-Vis spectroscopy, accompanied by assessments for sustained release, biocompatibility, and therapeutic efficacy. Through this pioneering approach, the incorporation of the anti-TB drug PYZ into the PYR-CSNP formulation was successfully achieved. The non-toxic profile of PYR-CSNP positions it as a compelling candidate for diverse biomedical applications, particularly in drug delivery for TB and other pathological conditions.

2. Methodology

2.1 Materials

Materials for synthesis included Chitosan (low molecular weight, 85% deacetylation) and pyrazinamide (99% purity) from Sigma Aldrich. Deionized water (resistivity: 18.20 $M\Omega cm^{-1}$), Sodium Tripolyphosphate (STPP) from Merck, Tween 80, and Acetic Acid (99.8%) from Hamburg Industries Inc. were used. Phosphate-buffered saline was from Sigma Aldrich. Chemicals were not purified further. Human normal lung fibroblast (MRC-5) cells were from the American Type Culture Collection (ATCC). Antimicrobial susceptibility testing involved Gram-negative bacteria (*E. coli and P.*

aeruginosa) and Gram-positive bacteria (*S. aureus and B. subtilis*), all from ATCC. All chemical reagents were of analytical grade, eliminating the need for additional purification. Solutions were prepared using distilled water, and glassware underwent cleaning with HNO3/HCl (3:1, v/v), followed by washing with double distilled water and drying before use.

2.2 Synthesis of Pyrazinamide-Loaded Chitosan Nanoparticles

In advancing drug delivery for anti-tuberculosis treatment, we systematically employed the ionic gelation method to synthesize Chitosan Nanoparticles (CS-NPs) loaded with Pyrazinamide. The goal was to enhance the therapeutic efficacy and targeted delivery of anti-tuberculosis agents. Pyrazinamide (PYR) was loaded into chitosan nanoparticles in separate batches, following a meticulous approach to maintain specificity and unique characteristics. The protocol involved preparing a solution with 2.0% (v/v) acetic acid, 0.5mg chitosan powder, and 0.3g of the drug, pre-dissolved in deionized water. Adjusting the chitosan solution's pH to 5 prevented agglomeration, with TWEEN-80 surfactant (2% v/v) ensuring stability. Simultaneously, a sodium tripolyphosphate (TPP) solution (7 mg/mL) was prepared in deionized water, with pH adjustment to 2. The gradual addition of TPP into the chitosan-drug solution (ratio 1:1.5 CS: TPP v/v), with continuous stirring, marked a crucial step in the ionic gelation process. Centrifugation at 4000 rpm separated the nanoparticles, followed by thorough washing and freeze-drying (Figure 1) [10].

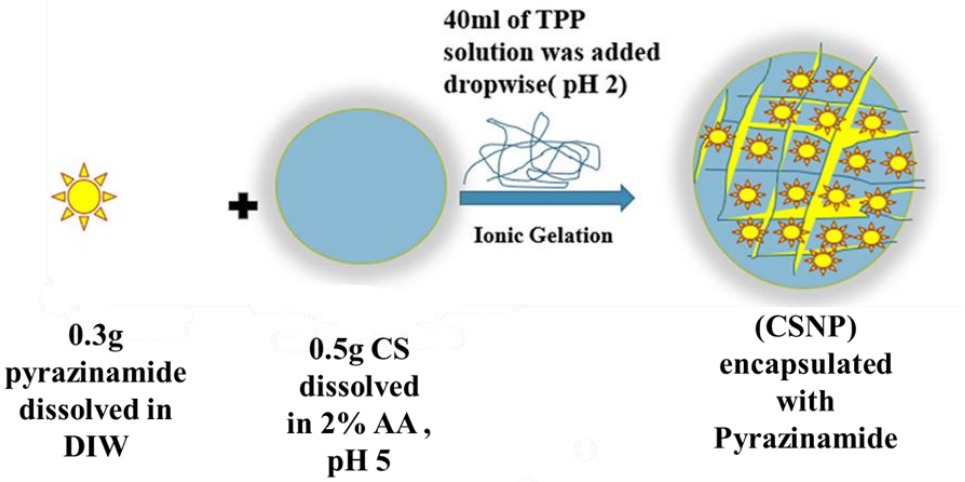

Fig. 1. Preparation chitosan nanoparticle encapsulated with pyrazinamide

This approach ensures the integrity of each drug-loaded formulation, contributing to pharmaceutical research in tailored drug delivery for anti-tuberculosis medications. The systematic synthesis lays the groundwork for further exploration and optimization, aiming for enhanced therapeutic outcomes [11].

2.3 Characterization

The PYR-CSNP underwent comprehensive characterization using diverse techniques. The Malvern high-performance dynamic light scattering (DLS) nano-sizer (UK) determined particle size distribution and polydispersity index (PDI). Drug release was measured with the Lambda ultraviolet-visible spectrophotometer from Perkin Elmer. X-ray diffraction (SHIMADZU XRD 6000, Japan) explored crystallinity patterns of PYR in PYR-CSNP nanoparticles. High-resolution transmission electron microscopy (HRTEM) (HITACHI H-7100, Japan) scrutinized nanoscale particle shape and dimensions.

Field emission scanning electron microscopy (FESEM) and Energy Dispersive X-Ray Spectroscopy (EDX) (NOVA NANOSEM, USA) investigated PYR-CSNP surface, morphology, and composition. Thermogravimetric and differential thermogravimetric (TGA/DTG) analyses (Mettler-Toledo Instrument, Switzerland) assessed thermal degradation. Fourier transform infrared spectroscopy (FTIR) (PerkinElmer FTIR spectrometer, SPECTRUM 1000) recorded PYR-CSNP and raw chitosan spectra. Experiments spanned 25-1000 °C with a 10 °Cmin−1 heating rate. The tested samples ranged from 6.0 to 8.0 mg.

2.4 Encapsulation Efficiency and Loading Capacity

UV-VIS Spectrophotometry was utilized for assessing the encapsulation efficiency and loading capacity of chitosan nanoparticles containing the pyrazinamide drug. The absorbance readings were taken at the specific PYR wavelength (λmax = 260 nm). For the analysis, 10 mg of powder samples were individually dissolved in a 10 mL buffer solution and agitated using an orbital shaker for approximately 3 hours. Subsequently, centrifugation at 4000 rpm was performed. A 2 mL volume of the supernatant was employed for absorbance measurement against a blank. The encapsulation efficiency (EE%) Eq. (1) and loading content (LC%) Eq. (2) of the samples were determined using the provided formulas [9].

$$\text{EE}\ (\%) = \frac{\text{Total nanoparticle with drug} - \text{Free drug}}{\text{Total nanoparticles with drug}} \times 100\% \quad (1)$$

$$\text{LC}\ (\%) = \frac{\text{The weight of drug in nanoparticles}}{\text{The weight of nanoparticles}} \times 100\% \quad (2)$$

2.5 In Vitro Anti-bacterial Study

The study investigated the antibacterial effectiveness of PYR-CSNPs against gram-positive and gram-negative bacteria, utilizing agar diffusion and broth dilution methods. Bacterial strains were cultured in Mueller-Hinton agar or broth (MHA or MHB) for 18 hours at 37 ℃. Disc diffusion tests were conducted on Escherichia coli, Pseudomonas aeruginosa, Staphylococcus aureus, and Bacillus subtilis. The bacterial suspension was grown in nutrient broth at 37 ℃ until reaching a density of 1.5 9108 CFU/mL. Discs loaded with varying CSNP concentrations were placed on nutrient agar plates, and kanamycin (30 µg/disk) served as a positive control. After 24 hours at 37 ℃, the inhibition zones were assessed. Each experiment was repeated three times for reliability.

2.6 MTT Cell Viability Assay

Cytotoxicity, the lethal impact of synthetic chemicals, natural toxins, or immune cells, is often evaluated through the MTT assay using 3-[4,5-dimethylthiazol-2-yl]-2,5-diphenyltetrazolium bromide. In our study, we used this method to assess the cytotoxicity of pure ATDs (such as Pyrazinamide), pure chitosan (CS), chitosan nanoparticles (CS-NPs), and PYR-CSNP. Human lung MRC-5 cells from ATCC were cultivated at a concentration of 4 x 103 cells/mL and exposed to various concentrations (500, 250, 125, 75, 25, 10, and 1 µg/mL) of the sample extracts for 72 hours [12]. After incubation, MTT solution was added, followed by three more hours of incubation. Optical density (OD) was measured at 570 nm after dissolving the formazan crystals in DMSO. The IC50 value, representing the drug concentration inhibiting 50% cell growth, was then calculated using a specific formula Eq. (3).

$$\text{Cell viability} = \frac{\text{Absorbance sample (mean)}}{\text{Absorbance control (mean)}} \times 100\% \quad (3)$$

3. Results

3.1 Size Optimization

Low molecular weight chitosan powder, chosen for its biodegradability and biocompatibility, was used to craft anti-TB drug-loaded nanoparticles. Ionic gelation between chitosan and TPP created crosslinks that physically entrapped the drug, with Tween 80 enhancing the particle surface. Concentration optimization revealed a 0.7 mg/mL TPP concentration yielding nanoparticles within the desired 50-150 nm size range [13]. Maintaining a pH of 5 prevented agglomeration. Increased TPP amounts were found to decrease particle size, emphasizing the need for precise concentration control for optimal drug delivery. Figure 2 illustrates the impact of TPP concentration on particle size and PDI.

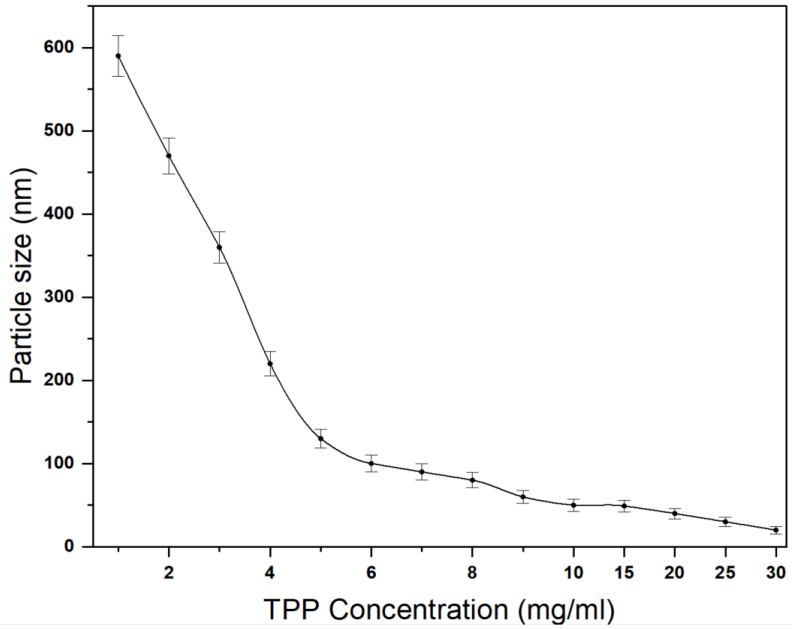

Fig. 2. The effect of TPP (mg/mL) on particle size (nm) and PDI index of chitosan NPs

The study washing underscores the importance of a lower drug ratio than chitosan for complete drug encapsulation and minimal losses. Table 1 detail size, PDI, % EE, and % LC based on the chitosan to anti-TB drug ratio, with UV-Vis spectroscopy revealing their dependency on chitosan polymer and drug concentrations [14].

Table 1
The effect of TPP (mg/mL) on particle size (nm) and PDI index of chitosan NPs

Samples	Chitosan: anti-TB drug ratio (mg/mL)	Size (nm) range	PDI range	EE % range	LC % range
CSNP- PYR loaded	5:0	10± 9.88	0.21	0.0 ± 0	0 ± 0
	5:1	20± 12.81	0.15	20.21 ± 1.21	7.71 ± 0.05
	5:2	30± 11.82	0.26	69.81 ± 3.32	12.22 ± 0.12
	5:3	40± 15.71	0.25	83.71 ± 2.41	18.22± 1.31
	5:4	50± 11.61	0.16	79.92 ± 1.92	14.81 ± 1.01
	5:5	20± 7.82	0.47	49.81 ± 0.91	7.61 ± 0.16
	5:6	15± 9.84	0.37	19.42± 1.32	6.93 ± 0.01
	5:7	20± 8.01	0.96	3.07 ± 1.14	12.94 ± 0.04
	5:8	10 ± 9.71	2.06	8.08 ± 0.52	6.02 ± 0.26
	1:3	15± 7.84	0.02	9.18 ± 0.61	1.91 ± 0.01
	2:3	40± 3.82	0.04	6.09 ± 0.92	8.91 ± 0.05
	4:3	60± 4.61	1.18	9.01 ± 1.12	3.22 ± 0.06
	6:3	20 ± 8.91	0.44	55.91 ± 2.63	12.9 ± 1.27
	7:3	10 ± 2.32	0.25	34.92 ± 2.35	14.24 ± 1.17
	8:3	10± 2.51	0.41	45.26 ± 1.91	9.59 ± 1.02
	9:3	5 ± 3.92	5.02	19.17 ± 1.21	6.19 ± 1.81

A higher chitosan percentage, interaction promotion, and maintaining a PDI within 0.2-0.3 are highlighted for nanoparticle stability (Figure 3).

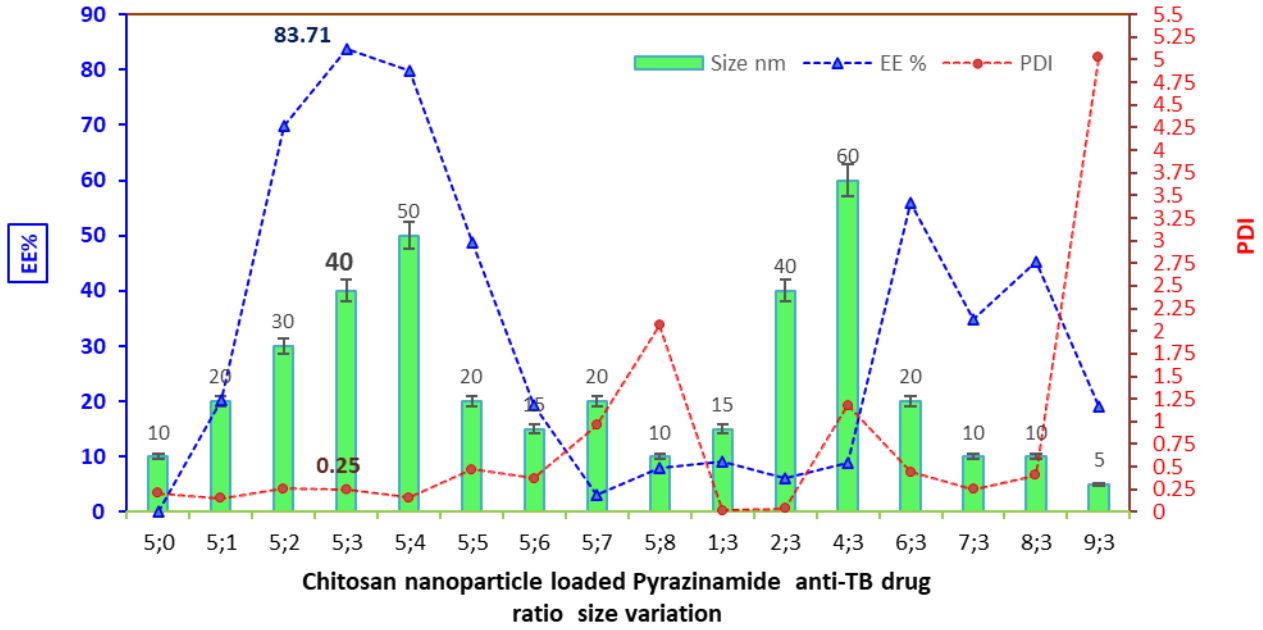

Fig. 3. Effect of the ratio of the CSNP loaded by Pyrazinamide on particle size, PDI and encapsulation efficiency NPs

3.2 Particle Size Distribution

The CS-PYR NPs exhibit a confined size range of 30-70 nm, with over 50% of particles at 40 nm or larger. The average size is 44 nm, consistent with hydrodynamic dimensions and HRTEM. Introducing the PYR drug increases the hydrodynamic mean diameter beyond pure chitosan NPs, ranging from 15-20 nm. Figure 4 shows a notably low PDI value of 0.25 for drug loaded CSNPs, well below the 0.05

threshold critical for DLS analysis. DLS-based size distributions confirm the suitability of synthesized CS-PYR nanoparticles for drug delivery, highlighting their appropriately small sizes [15].

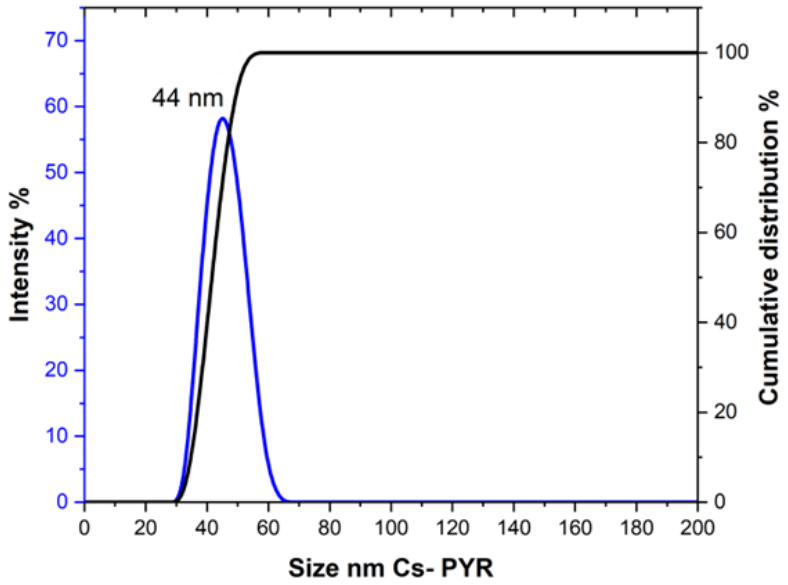

Fig. 4. Relative and cumulative particles size distribution of chitosan nanoparticle loaded with pyrazinamide

3.3 High-Resolution Transmission Electron Micrograph

The CS-PYR NPs exhibit a confined size range HR-TEM analysis indicated in Figure 5, confirmed the size and distribution of Pyrazinamide-loaded chitosan nanoparticles. Image software analysed 30 randomly selected CS-PYR-NPs from the TEM image, revealing sizes ranging from 30 to 70 nm. The mean size was 45.71 nm, with a standard deviation of 3.52 nm. The figure illustrates uniformly dispersed, spherical CS-PYR-NPs. Compared to pure CS-NPs, drug-loaded NPs were larger, indicating successful drug incorporation. While most nanoparticles showed separation, occasional agglomeration occurred, possibly due to surface energy. Nonetheless, these nanoparticles in the specified size range demonstrate favourable characteristics for drug delivery, extending their bloodstream longevity [16].

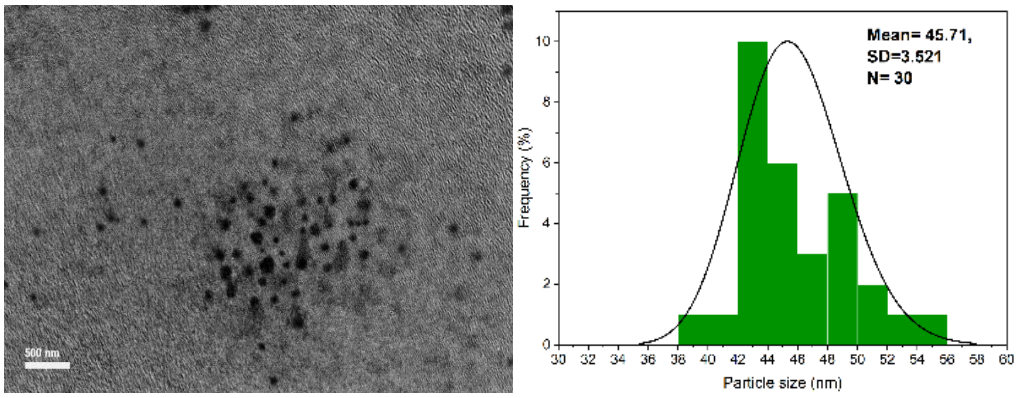

Fig. 5. TEM of chitosan nanoparticle loaded with pyrazinamide

3.4 Surface Properties using the Field Emission Scanning Electron Microscopy and Qualitative Elemental Analysis Using Energy Dispersive X-Ray

In Figure 6, the surface characteristics of Pyrazinamide-loaded chitosan nanoparticles PYR-CSNP and their energy dispersive spectroscopy (EDS) analysis are shown. The PYR-CSNP, with a size of about 30–50 nm, exhibit a uniform and smooth surface. The slight increase in size indicates successful drug loading, with the particles maintaining a spherical shape and minimal aggregation, presenting a consistent and homogeneous structure.

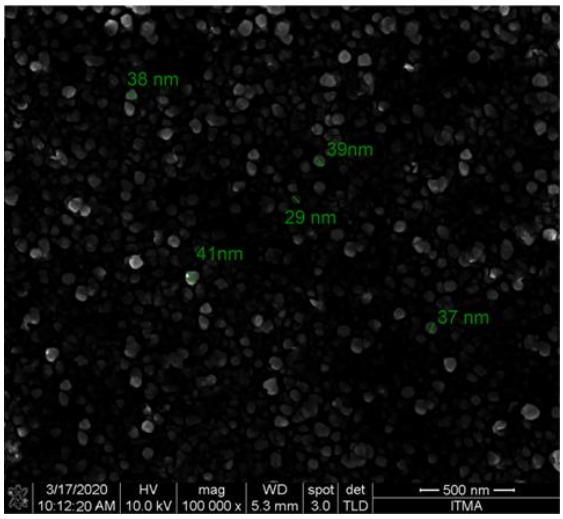

Fig. 6. FESEM of chitosan nanoparticle loaded with pyrazinamide

Table 2 and Figure 7, accordingly outlines the EDX elemental composition, presenting weight and atomic percentages for all samples. During EDX measurement, different regions were examined to determine elemental contents. In each sample, elements C, N, P, O, and Na were identified (Figure 7). Carbon levels peaked between 0.2-0.3 keV, and oxygen was consistently present, crucial for CSNP and PYR. CS-PYR nanoparticles displayed weight percentages of C, N, O, P, and Na, with notable sodium attributed to the crosslinking process involving sodium tripolyphosphate. In the EDX heating process, the nitrogen peak around 0.4 keV remains unidentified due to overlap with the consistently observed oxygen peak at 0.5 keV, resulting in its exclusion from the results [16].

Table 2
Elemental compositions: atomic and weight (%) of the nanoparticles obtained by the EDX analysis

Atomic & Weight %	Element (%)	CS-PYR NPs	CS-NPs
Atomic %	P	20.22	34.49
	N	1.49	1.52
	O	58.28	50.18
	NA	10.77	7.66
	C	5.29	5.88
Weight %	P	28.19	27.25
	N	3.35	2.66
	O	41.49	39.23
	NA	14.74	14.77
	C	10.38	13.96

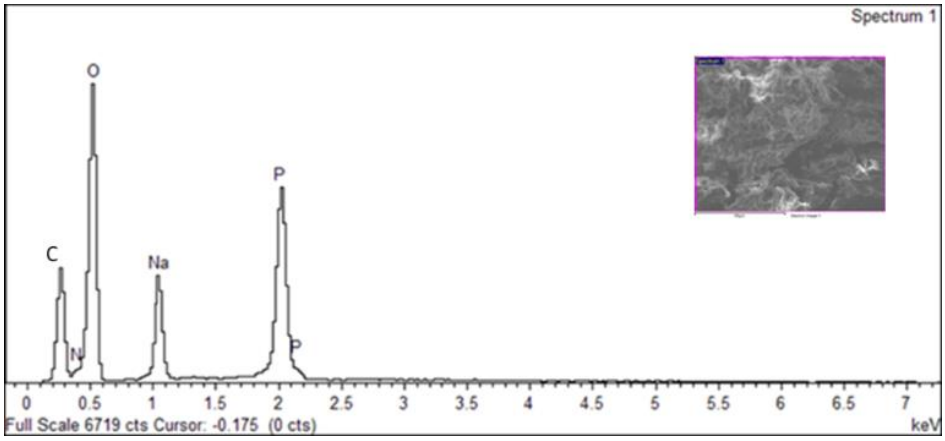

Fig. 7. EDX spectrum of chitosan-loaded pyrazinamide NPs

3.5 X-Ray Diffraction

According to Figure 8 XRD data, CSNPs exhibit a broad peak, indicating their amorphous nature. Conversely, untreated PYR displays clear crystalline peaks at 2θ angles of 18, 21, and 37°, confirming the presence of PYR crystals. Under ion gelation conditions, CSNPs show crystalline peaks at 2θ = 22.5° and two sharp reflections between 2θ = 35-50°, associated with the main peak of CsNPs. These two sharp reflections in PYR-loaded CSNPs suggest the physical state of the chitosan matrix when loaded with PYR. The distinctive sharp peaks for PYR mostly diminish in the diffractogram of Cs-PYR nanoparticles [17]. However, the light intensity of both Cs and drug characteristic peaks is noticeable in CS-PYR NPs. The PYR peak at 2θ = 37° is less pronounced in CS-PYR NPs, likely due to chitosan encapsulation. These diffuse peaks with low intensities confirm PYR encapsulation and suggest the amorphous nature of CS-PYR NPs [9].

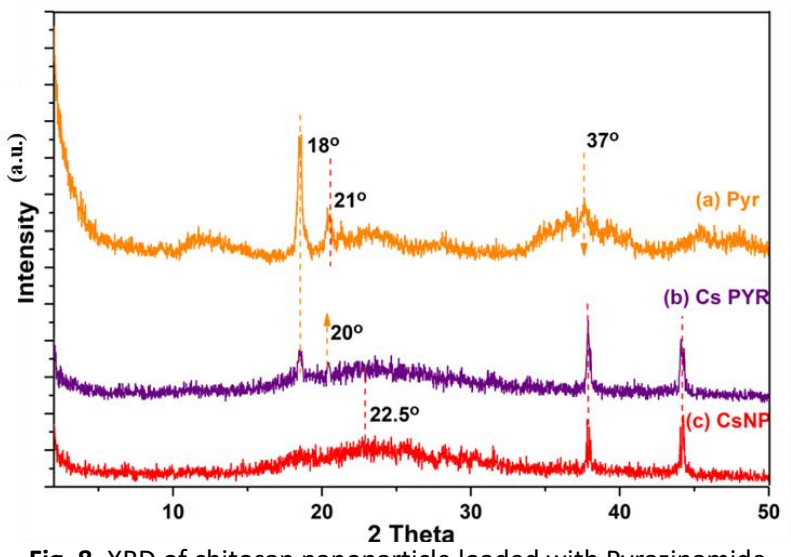

Fig. 8. XRD of chitosan nanoparticle loaded with Pyrazinamide

3.6 Transform Infrared Spectroscopy

Pyrazinamide-loaded chitosan underwent IR analysis to confirm PYR integration as shown in Figure 9. CSNP, absorption bands were observed at 3,300-3, 400 cm^{-1} (OH stretching and N-H stretching), and 2900 cm^{-1} (C-H stretching). Amide I and amide II peaks were present at 1627 cm^{-1}

(C=O stretching) and 1529 cm^{-1} (N-H in-plane deformation coupled with C≡N stretching). Additional peaks appeared at 1156 cm^{-1} (bridge –O- stretching) and 1062 cm^{-1} (-CO stretching). In the free drug FTIR spectrum, characteristic amine group vibrations occurred at 3402 cm^{-1} (asymmetric) and 3285 cm^{-1} (symmetric). PYR spectrum displayed peaks at 1701 cm^{-1} (amide I) and 1402 cm^{-1} (amide II), with the carbonyl (C=O) stretching band at 1500-500 cm^{-1}.

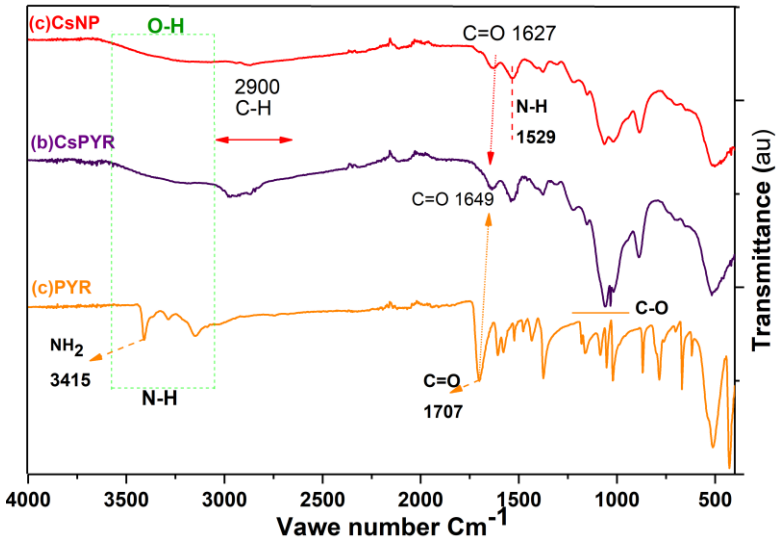

Fig. 9. FTIR of chitosan nanoparticle-loaded with pyrazinamide

CS-PYR NPs IR spectrum (Figure 9) exhibited characteristic PYR absorption bands. NH_2 bands at 3415 cm^{-1} for PYR were observed around 4000-3500 cm^{-1} in CS-PYR NPs. Amine and carboxyl groups of PYR appeared in the 1600-1000 cm^{-1} range, matching CS-PYR NPs. FTIR of CS-PYR NPs showed vibrational bands for PYR and CSNP with slight shifts [9]. The presence of characteristic functional group bands from both PYR and CS in CS-PYR NPs aligned with XRD results, confirming successful PYR intercalation [18]. Vibration bands details for CS-PYR NPs are provided in Table 3.

Table 3
FTIR bands of functional groups of CS-NPs, free PYR & CS-PYR NPs

Bands	CS-NPs cm^{-1}	PYR cm^{-1}	CS-PYR cm^{-1}
N-H stretching	2900	4000 - 3500	4000 - 3500
O-H stretching	3,000-3500	3,000-3500	3,000-3500
C=C	1500-1000	1500-500	1500-500
C=N	-	-	1606
Aromatic C-C stretching	1500-1300	1500-1300	1500-1300
C-O stretching	1500-500	1500-500	1500-500
C-H bending	700-900	2900	
O-H bending of Carboxylic acid group	1600-1000	1600-1000	1600-1000

3.7 Thermogravimetric Analysis

Thermograms depicting the weight loss curve as temperature increases for the synthesized CS-PYR NPs, analysed in a nitrogen gas flow that indicated in Figure 10. CS-PYR NPs exhibit two weight loss stages at 74-164°C (16.8% mass loss) and 164-560°C (34.7% mass loss). The first stage involves water molecule release and chitosan decomposition via hydrogen bond loss, while the second stage includes the release of H_2O, NH_3, CO, CO_2, and CH_3COOH from PYR drug decomposition [16]. This

aligns with earlier chitosan nanoparticle investigations, associating such weight loss with water desorption. The temperature range suggests the water is loosely bonded to the chitosan surface. Subsequently, CH4 release occurs at 800–1000°C, causing a modest 15.7 wt.% weight loss [9]. Thus, CS-PYR NP experiences two weight loss phases: initial loss due to physically adsorbed water and subsequent thermal decomposition of the PYR drug with dihydroxylation.

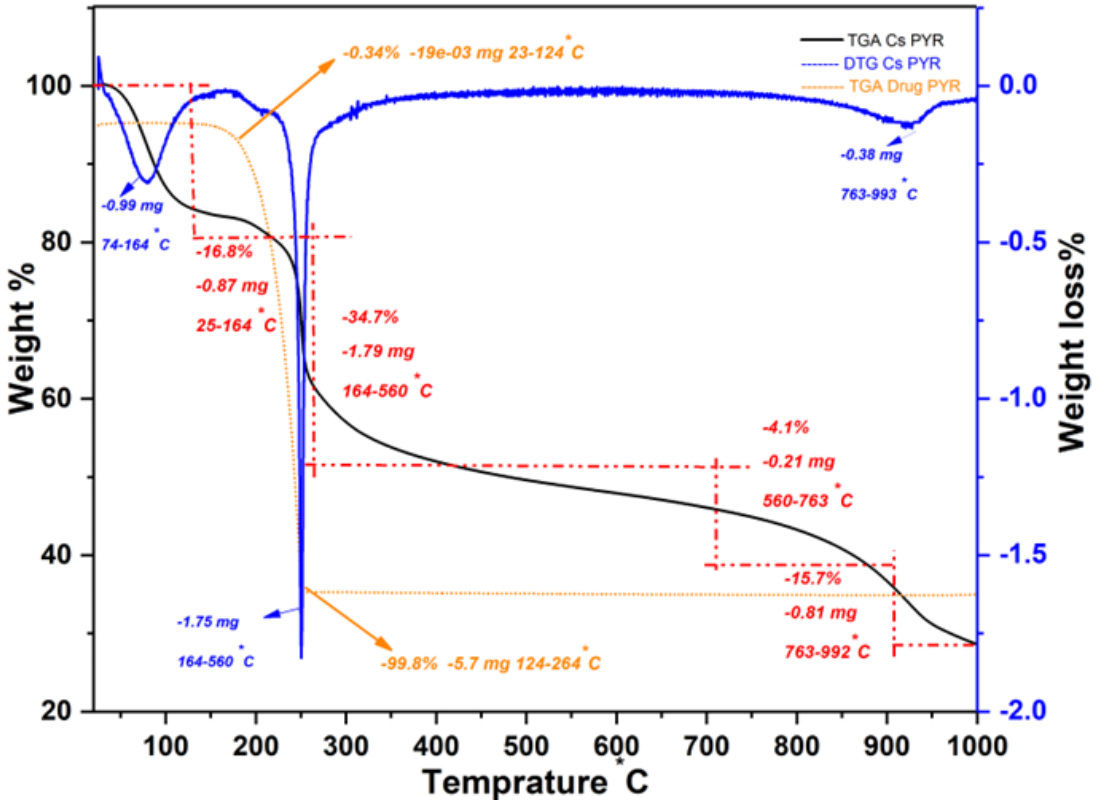

Fig. 10. TGA of chitosan nanoparticle loaded with pyrazinamide

3.8 The In Vitro Drug Release Study

The Encapsulation Efficiency, Loading Content of pyrazinamide loaded chitosan nanoparticles shown in Table 4. The results showed effective encapsulation and loading of drugs in all sample. The release of Pyrazinamide-loaded chitosan nanoparticles, detailed in Table 4 and Figure 11, exhibits a disciplined pattern with gradual release at pH 4.8 and a subsequent burst at pH 7.4. Within the initial 7 days, anti-TB drug release peaks at 90-100% in acidic (pH 4.8) conditions and 80-90% in neutral (pH 7.4) environments. This pH-responsive behaviour ensures targeted drug release at the infection site, crucial for optimal therapeutic concentrations while minimizing systemic exposure and potential side effects [12]. The nanoparticles demonstrate controlled and sustained drug release, evident in the absence of burst release and the observed release rates in the critical initial days [19]. The chitosan-tripolyphosphate crosslinked structure contributes to these mechanisms. Combined with chitosan's mucoadhesive properties, the pH-responsive nature positions these nanoparticles for effective navigation in the lung environment, ensuring prolonged contact with lung epithelium and enhanced drug absorption [18]. The release data not only confirms pH responsiveness but also establishes a clear connection between distinctive release profiles and the potential of these nanoparticles as an effective drug delivery system for targeted treatment of pulmonary tuberculosis, solidifying their innovative role in TB therapeutics.

Table 4
The PYR-CSNP percentages of loading-content, encapsulation-efficiency and the drug release in PBS in acidic and alkaline pH at 120 hours

Sample	Loading-Content (%)	Encapsulation Efficiency (%)	Release % in pH 4.8	Release % in pH 7.4
PYR-CSNP	27.25± 1.52	85.19 ± 2.51	99.23	85.34

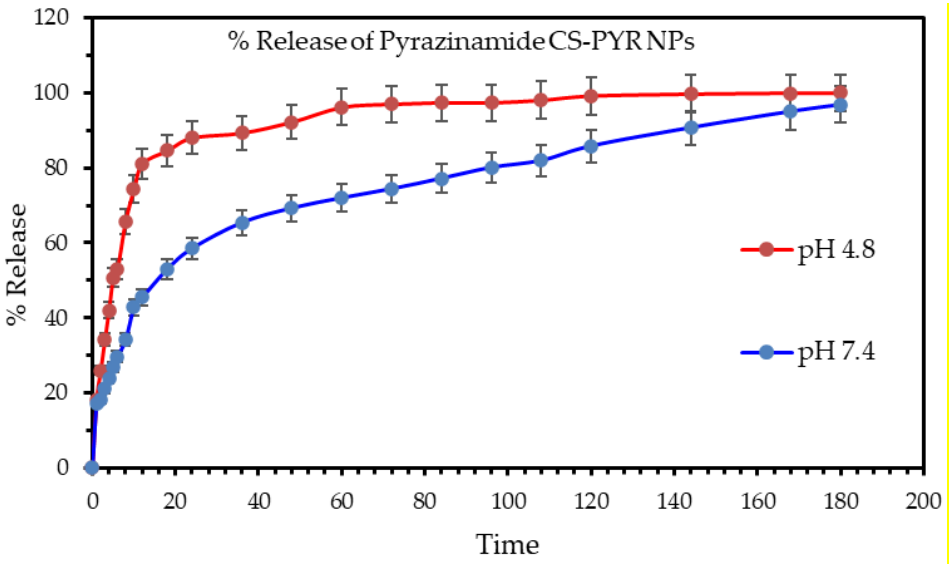

Fig. 11. Release of pyrazinamide from CS-PYR NPs sample in phosphate-buffered solutions at pH 4.8 and pH 7.4

3.9 Antibacterial Study

The antibacterial screening of pyrazinamide (PYR)-loaded chitosan nanoparticles (NPs) against Gram-negative (*E. coli* and *P. aeruginosa*) and Gram-positive (*S. aureus* and *B. subtilis*) bacteria was conducted using disc diffusion assays (Figure 12). Once inside bacterial cells, the CSNPs undergo degradation, releasing PYR, which interferes with cell wall biosynthesis. The released PYR exerts antibacterial activity, disrupting essential cellular processes and inhibiting bacterial growth. In disc diffusion assays, PYR-loaded CSNPs create inhibition zones, reflecting the extent of bacterial growth inhibition. The pH-responsive behaviour of CS contributes to effective drug release, with a higher release rate under acidic conditions, aligning with the acidic bacterial cell environment. The sustained drug release potential of the chitosan matrix and adaptability to dynamic pH variations within the respiratory tract enhance the targeted drug delivery and efficacy [20].

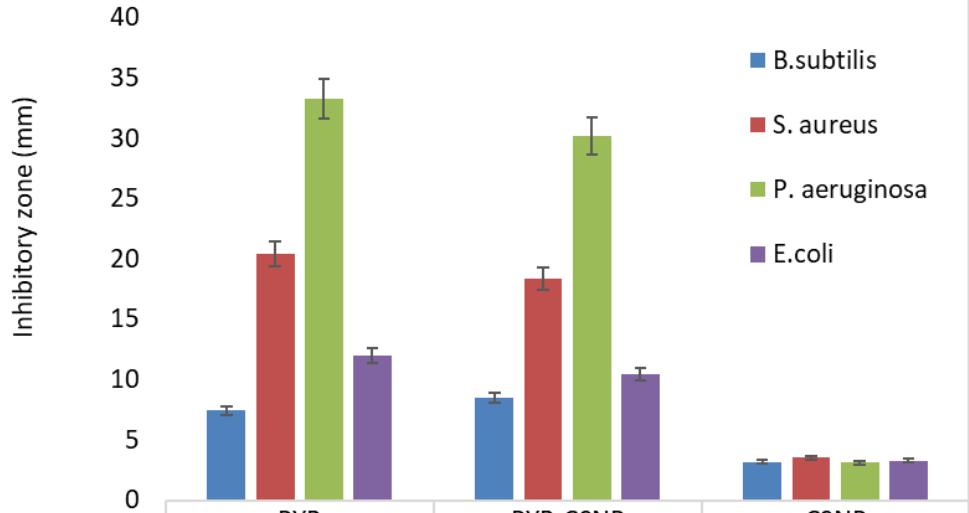

	PYR	PYR-CSNP	CSNP
B.subtilis	7.41	8.48	3.18
S. aureus	20.43	18.35	3.52
P. aeruginosa	33.28	30.18	3.12
E.coli	12	10.47	3.29

Fig. 12. Inhibitory zone estimation for repurposing of pyrazinamide loaded CSNPs for antibacterial activities on selected bacteria (*S. aureus, B. subtilis, E. coli and P. aeruginosa*)

PYR-loaded chitosan nanoparticles offer a promising platform for targeted treatment against a range of bacteria, including those resembling Mycobacterium tuberculosis. Using bacterial tests as a safer alternative to direct evaluation of Mycobacterium tuberculosis is motivated by safety concerns and the need for specialized facilities. Employing established gram-positive and gram-negative strains in antibacterial assays provides a practical and secure approach for preliminary assessments, ensuring methodological rigor and facilitating a broader evaluation of chitosan-loaded drug formulations. The observed antibacterial activity forms a foundation for further investigation into the specific mechanisms underlying the efficacy of chitosan-loaded drugs against Mycobacterium tuberculosis [7,21].

In a nutshell, based on the comprehensive antibacterial screening conducted against Gram-negative (*E. coli* and *P. aeruginosa*) and Gram-positive (*S. aureus* and *B. subtilis*) bacterial strains, it is evident that the chitosan nanoparticle-loaded pyrazinamide system demonstrates significant efficacy in inhibiting bacterial growth. Moreover, the strategic selection of these bacterial models, with their diverse cell wall characteristics and physiological similarities to Mycobacterium tuberculosis, offers a valid simulation for assessing the potential efficacy of targeted drug delivery in lung infections. Additionally, the pH-responsive behaviour of the nanocarrier, facilitating drug release in acidic conditions resembling the lung microenvironment, pH-responsive drug release mechanism ensures targeted delivery of PYR, enhancing its efficacy against intracellular pathogens like MTB which is further supports its suitability for targeted drug delivery to infected lung tissues [24]. This approach ensures methodological rigor and facilitates insights into the potential of chitosan nanoparticle-mediated drug delivery in addressing lung infections, without the complexities associated with direct Mycobacterium tuberculosis testing. In light of these considerations, the decision to prioritize antibacterial testing against commonly used bacterial strains serves as a strategic approach to lay the groundwork for future investigations into the specific mechanisms underlying the efficacy of

chitosan-loaded drugs against Mycobacterium tuberculosis. This approach ensures methodological rigor, minimizes safety risks associated with handling pathogenic strains, and paves the way for subsequent studies to explore the translation of findings to clinically relevant models of TB infection.

3.10 Vitro Cytotoxicity Study of Normal Human Lung Cells (MRC-5)

In Figure 13, MRC-5 cell viability after a 72-hour incubation shows minimal cytotoxicity of the samples. The empty carriers CS and CS-NPs are non-toxic to healthy lung cells, suitable for nanocarrier formulation. Conversely, naked drug PYR exhibit significant dose- and time-dependent toxic effects on MRC-5 cells. At the highest concentration (500 µg/mL) after 72 hours, free drug result in about 40% cell viability and 60% cell death, while the nanocarrier demonstrates 80% cell viability and 20% cell death [22]. This suggests that the synthesized nanocarrier formulations are more biocompatible at higher concentrations, making them suitable for TB treatment without harming healthy cells. Importantly, there is no significant difference in cell death when the drug is loaded into nanocarriers, indicating the effectiveness of all formulations for treating TB compared to free drugs [23].

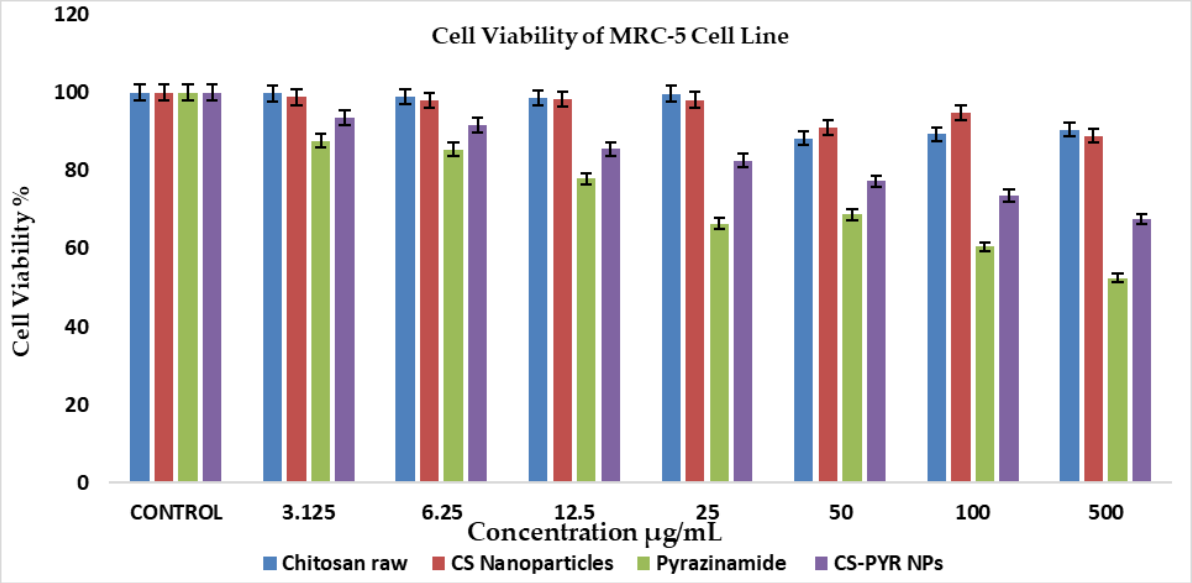

Fig. 13. Cytotoxicity assay of pure CS, CS-NPs, pyrazinamide, and CS-PYR NPs, against MRC-5 normal lung cells at 72 h of incubation. Values are expressed as mean ± SD of triplicates. The significant differences ($p < 0.05$) * were determined on MRC-5 cell using the one-way ANOVA followed by Duncan's multiple range test

4. Conclusions

This study successfully prepared Pyrazinamide (PYR) drug-loaded chitosan nanoparticles (CSNP) via ionic gelation and chemical crosslinking of tripolyphosphate (TPP). Characterization techniques validated the distinctive properties of the formulation, revealing spherical morphology with an average diameter of 40-70 nm. The drug-loaded CSNP exhibited sustained release, superior antibacterial activity, and 80% cell viability in MRC5 cells, showcasing its biocompatibility. PYR loading in CSNP emerges as a promising strategy for enhanced treatment efficacy, reduced risk of drug resistance/toxicity, and targeted, sustained drug release, positioning PYR-CSNP as a safe and effective nanodelivery system for TB treatment and representing a significant advancement in therapeutic outcomes.

5. Future Aspects

Future investigations in the realm of protein and gene delivery ought to prioritize the refinement of chitosan nanoparticle formulations loaded with antitubercular drugs for optimal efficiency, while concurrently evaluating their biocompatibility. Concurrently, emphasis should be placed on elucidating targeted delivery strategies tailored towards specific cellular or tissue targets, thereby augmenting therapeutic efficacy. Moreover, prospective research endeavours should encompass the exploration of the application of drug loaded nanoparticles within animal models and clinical trials to meticulously evaluate their therapeutic efficacy and safety profiles. The optimization of formulation and manufacturing processes stands as a pivotal avenue to not only bolster the performance but also scale the nanodelivery system, thus facilitating its seamless integration into clinical practice.

Acknowledgement

The author would like to express sincere gratitude to the university Putra Malaysia for the characterizations supports and the staffs and the UPM institute of bio since (IBS). Gran Putra Berimpak provided funding for this work.

Disclosure

No conflicts of interest have been disclosed by the authors for this research

References

[1] Primo, Laura Maria Duran Gleriani, Cesar Augusto Roque-Borda, Christian Shleider Carnero Canales, Icaro Putinhon Caruso, Isabella Ottenio de Lourenço, Vitória Maria Medalha Colturato, Rafael Miguel Sábio et al. "Antimicrobial peptides grafted onto the surface of N-acetylcysteine-chitosan nanoparticles can revitalize drugs against clinical isolates of Mycobacterium tuberculosis." *Carbohydrate Polymers* 323 (2024): 121449. https://doi.org/10.1016/j.carbpol.2023.121449

[2] Yusefi, Mostafa, Kamyar Shameli, Michiele Soon Lee-Kiun, Sin-Yeang Teow, Hassan Moeini, Roshafima Rasit Ali, Pooneh Kia, Chia Jing Jie, and Nurul Hidayah Abdullah. "Chitosan coated magnetic cellulose nanowhisker as a drug delivery system for potential colorectal cancer treatment." *International journal of biological macromolecules* 233 (2023): 123388. https://doi.org/10.1016/j.ijbiomac.2023.123388

[3] Kia, Pooneh, Umme Ruman, Ariyati Retno Pratiwi, and Mohd Zobir Hussein. "Innovative therapeutic approaches based on nanotechnology for the treatment and management of tuberculosis." *International journal of nanomedicine* (2023): 1159-1191. https://doi.org/10.2147/IJN.S364634

[4] Yusefi, Mostafa, Hui-Yin Chan, Sin-Yeang Teow, Pooneh Kia, Michiele Lee-Kiun Soon, Nor Azwadi Bin Che Sidik, and Kamyar Shameli. "5-fluorouracil encapsulated chitosan-cellulose fiber bionanocomposites: synthesis, characterization and in vitro analysis towards colorectal cancer cells." *Nanomaterials* 11, no. 7 (2021): 1691. https://doi.org/10.3390/nano11071691

[5] Varma, JN Ravi, T. Santosh Kumar, B. Prasanthi, and J. Vijaya Ratna. "Formulation and characterization of pyrazinamide polymeric nanoparticles for pulmonary tuberculosis: Efficiency for alveolar macrophage targeting." *Indian journal of pharmaceutical sciences* 77, no. 3 (2015): 258. https://doi.org/10.4103/0250-474X.159602

[6] Saifullah, Bullo, Alina Chrzastek, Arundhati Maitra, Bullo Naeemullah, Sharida Fakurazi, Sanjib Bhakta, and Mohd Zobir Hussein. "Novel anti-tuberculosis nanodelivery formulation of ethambutol with graphene oxide." *Molecules* 22, no. 10 (2017): 1560. https://doi.org/10.3390/molecules22101560

[7] Singh, Richa, Surya Prakash Dwivedi, Usha Singh Gaharwar, Ramovatar Meena, Paulraj Rajamani, and Tulika Prasad. "Recent updates on drug resistance in Mycobacterium tuberculosis." *Journal of applied microbiology* 128, no. 6 (2020): 1547-1567. https://doi.org/10.1111/jam.14478

[8] Changsan, Narumon, and Chutima Sinsuebpol. "Dry powder inhalation formulation of chitosan nanoparticles for co-administration of isoniazid and pyrazinamide." *Pharmaceutical development and technology* 26, no. 2 (2021): 181-192. https://doi.org/10.1080/10837450.2020.1852570

[9] Saifullah, Bullo, Palanisamy Arulselvan, Sharida Fakurazi, Thomas J. Webster, Naeemullah Bullo, Mohd Zobir Hussein, and Mohamed E. El Zowalaty. "Development of a novel anti-tuberculosis nanodelivery formulation using

magnesium layered hydroxide as the nanocarrier and pyrazinamide as a model drug." *Scientific Reports* 12, no. 1 (2022): 14086. https://doi.org/10.1038/s41598-022-15953-6

[10] Maluin, Farhatun Najat, Mohd Zobir Hussein, Nor Azah Yusof, Sharida Fakurazi, Abu Seman Idris, Nur Hailini Zainol Hilmi, and Leona Daniela Jeffery Daim. "Preparation of chitosan–hexaconazole nanoparticles as fungicide nanodelivery system for combating Ganoderma disease in oil palm." *Molecules* 24, no. 13 (2019): 2498. https://doi.org/10.3390/molecules24132498

[11] Ruman, Umme, Kalaivani Buskaran, Saifullah Bullo, Georgia Pastorin, Mas Jaffri Masarudin, Sharida Fakurazi, and MOHD ZOBIR HUSSEIN. "Sorafenib and 5-Fluorouracil Loaded Dual Drug Nanodelivery Systems for Hepatocellular Carcinoma and Colorectal Adenocarcinoma." (2021). https://doi.org/10.21203/rs.3.rs-152602/v1

[12] Barahuie, Farahnaz, Dena Dorniani, Bullo Saifullah, Sivapragasam Gothai, Mohd Zobir Hussein, Ashok Kumar Pandurangan, Palanisamy Arulselvan, and Mohd Esa Norhaizan. "Sustained release of anticancer agent phytic acid from its chitosan-coated magnetic nanoparticles for drug-delivery system." *International journal of nanomedicine* (2017): 2361-2372. https://doi.org/10.2147/IJN.S126245

[13] Yusefi, Mostafa, Pooneh Kia, Siti Nur Amalina Mohamad Sukri, Roshafima Rasit Ali, and Kamyar Shameli. "Synthesis and properties of chitosan nanoparticles crosslinked with tripolyphosphate." *Journal of Research in Nanoscience and Nanotechnology* 3, no. 1 (2021): 46-52. https://doi.org/10.37934/jrnn.3.1.4652

[14] Valentino, Anna, Raffaele Conte, Ilenia De Luca, Francesca Di Cristo, Gianfranco Peluso, Michela Bosetti, and Anna Calarco. "Thermo-responsive gel containing hydroxytyrosol-chitosan nanoparticles (Hyt@ tgel) counteracts the increase of osteoarthritis biomarkers in human chondrocytes." *Antioxidants* 11, no. 6 (2022): 1210. https://doi.org/10.3390/antiox11061210

[15] Kushwaha, Kalpana, and Harinath Dwivedi. "Interfacial phenomenon based biocompatible alginate-chitosan nanoparticles containing isoniazid and pyrazinamide." *Pharmaceutical Nanotechnology* 6, no. 3 (2018): 209-217. https://doi.org/10.2174/2211738506666180625120038

[16] Banat, Heba, Ildikó Csóka, Dóra Paróczai, Katalin Burian, Árpád Farkas, and Rita Ambrus. "A Novel Combined Dry Powder Inhaler Comprising Nanosized Ketoprofen-Embedded Mannitol-Coated Microparticles for Pulmonary Inflammations: Development, In Vitro–In Silico Characterization, and Cell Line Evaluation." *Pharmaceuticals* 17, no. 1 (2024): 75. https://doi.org/10.3390/ph17010075

[17] Krisanti, Elsa Anisa, Talitha Zada Gofara, Ahmad Jabir Rahyussalim, and Kamarza Mulia. "Polyvinyl alcohol (PVA)/chitosan/sodium tripolyphosphate (STPP) hydrogel formulation with freeze-thaw method for anti-tuberculosis drugs extended release." In *AIP Conference Proceedings*, vol. 2370, no. 1. AIP Publishing, 2021. https://doi.org/10.1063/5.0063175

[18] Gunasekaran, S., and E. Sailatha. "Vibrational analysis of pyrazinamide." (2009).

[19] Maral, Alka, Pooja Gupta, Prerna Gupta, and Alok Semwal. "FORMULATION AND EVALUATION OF CHITOSAN MICROSPHERES OF COMBINED DRUG (ISONIAZID AND PYRIDOXINE) RELEASE PROFILE BY IONOTROPIC GELATION METHOD." *Journal of Population Therapeutics and Clinical Pharmacology* 30, no. 18 (2023): 1134-1145.

[20] Chen, Hongyu, Wei Tan, Tianyi Tong, Xin Shi, Shiqing Ma, and Guorui Zhu. "A pH-responsive asymmetric microfluidic/chitosan device for drug release in infective bone defect treatment." *International Journal of Molecular Sciences* 24, no. 5 (2023): 4616. https://doi.org/10.3390/ijms24054616

[21] Shi, Xiaoxin, Rajendran Amarnath Praphakar, Kannan Suganya, Marudhamuthu Murugan, Perumal Sasidharan, and Mariappan Rajan. "In vivo approach of simply constructed pyrazinamide conjugated chitosan-g-polycaprolactone micelles for methicillin resistance Staphylococcus aureus." *International journal of biological macromolecules* 158 (2020): 636-647. https://doi.org/10.1016/j.ijbiomac.2020.04.214

[22] Khan, Yelena A., Kadir Ozaltin, Andres Bernal-Ballen, and Antonio Di Martino. "Chitosan-alginate hydrogels for simultaneous and sustained releases of ciprofloxacin, amoxicillin and vancomycin for combination therapy." *Journal of Drug Delivery Science and Technology* 61 (2021): 102126. https://doi.org/10.1016/j.jddst.2020.102126

[23] Manca, Maria-Letizia, Spyridon Mourtas, Vassileios Dracopoulos, Anna Maria Fadda, and Sophia G. Antimisiaris. "PLGA, chitosan or chitosan-coated PLGA microparticles for alveolar delivery?: A comparative study of particle stability during nebulization." *Colloids and Surfaces B: Biointerfaces* 62, no. 2 (2008): 220-231. https://doi.org/10.1016/j.colsurfb.2007.10.005

[24] Kucukoglu, Vildan, Huseyin Uzuner, Halime Kenar, and Aynur Karadenizli. "In vitro antibacterial activity of ciprofloxacin loaded chitosan microparticles and their effects on human lung epithelial cells." *International Journal of Pharmaceutics* 569 (2019): 118578. https://doi.org/10.1016/j.ijpharm.2019.118578